THESSALONIKI SEISMIC HAZARD ASSESSMENT: PROBABILISTIC AND DETERMINISTIC APPROACH FOR ROCK SITE CONDITIONS

K. Pitilakis[1], G. Cultrera[2], B. Margaris[3], G. Ameri[2], A. Anastasiadis[1], G. Franceschina[2] and S. Koutrakis[4]

ABSTRACT

Within the framework of four research projects (RISK-EU, EUROSEISRISK, SRM_LIFE and LESSLOSS) extensive calculations were carried out assessing the seismic hazard in the Thessaloniki and surrounding area. The main results were derived from probabilistic and deterministic approaches taking into account rock site conditions for each examined site in the Metropolitan area of Thessaloniki. The expected strong-ground motions were calculated applying different methodologies. Two different groups worked for the assessment of the seismic hazard, the first one constituted of the INGV (Istituto Nazionale di Geofisica e Vulcanologia, Italy) and LSMF (Laboratory of Soil Mechanics and Foundation Engineering, Thessaloniki, Greece) and the second one of LSMF and ITSAK (Institute of Engineering Seismology and Earthquake Engineering, Thessaloniki, Greece).

Keywords: Probabilistic, deterministic, seismic hazard, strong motion synthetics.

INTRODUCTION

Safety against earthquake hazard potential has two main aspects, structural safety against earthquake dynamic loading and the safety of a site itself related to geotechnical potential phenomena such as amplifications, landslides etc. For this reason, seismic zoning is one of the most fundamental aspects of seismic hazard assessment and the estimation of future strong ground motions. Earthquake ground motions are affected by several factors such as seismic sources (regional/ local seismicity), propagation path (attenuation of ground motion) and site effects (local site and geological conditions).

The seismotectonic model adopted combines faults and background area sources. The geometries of the faults were proposed from Papazachos et al. (2001). These are the faults that are responsible for all historical earthquakes (with a magnitude M>6) that occurred in Greece from the 5th century BC till present. The seismotectonic data (seismicity rates, b parameter, M_{max} values, etc.), were defined by Papaioannou and Papazachos (2000) for Greece. The background seismicity of the area sources used has been defined by Karakaisis (personal communication) and has been accounted for earthquakes with magnitudes between 4.0 and 5.9 proposing finally 12 area sources in Greece. Only faults and background area sources at a distance of 150 kilometers or less has been included. The studied area along with the two sites of specific interest and the neighboring faults are shown in Figure 1.
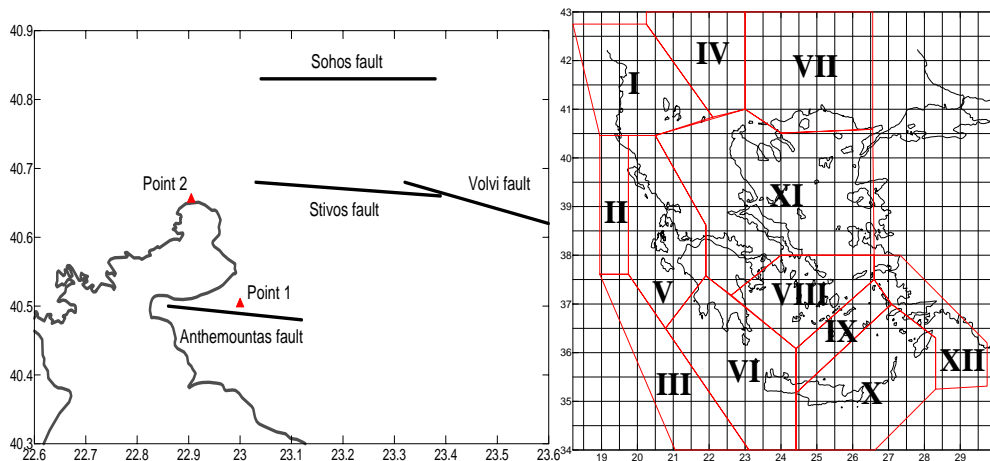
[1] Department of Civil Engineering, Aristotle University of Thessaloniki, Greece.
[2] Istituto Nazionale di Geofisica e Vulcanologia, INGV, Italy.
[3] Institute of Engineering Seismology and Earthquake Engineering, ITSAK, Greece.
[4] MSc Geophysicist, Department of Geophysics, University of Thessaloniki, Greece.

Figure 1. Study area, sites of interest (points 1 and 2), neighboring faults (left) and background area sources (right)

In this paper, an analytical description of the assessment of seismic hazard for the area of Thessaloniki is presented, based on the two different approaches proposed by the two working groups examining two specific sites in the Metropolitan area of Thessaloniki. The first site is located in downtown Thessaloniki (point 1, 22.999E-40.503N) and the other one in the eastern part of the area studied, near Anthemountas seismic fault (point 2, 22.905E-40.648N). The estimation of strong motion was carried out taking into consideration rock site conditions for both sites. Comparison and discussion of the results were attempted considering the different approaches applied by the two working groups.

## GROUND SHAKING SCENARIOS

Probabilistic Approach

Peak ground acceleration (PGA), is the strong ground motion parameter for which the calculations were performed. The empirical predictive relations that were used, are the ones proposed by Skarlatoudis et al., (2003). Figure 2 shows the results of the probabilistic seismic hazard analysis for the studied area for two different values of return period, 50 and 475 years.

Figure 3 is shows the contributions to the PGA hazard of the faults and background seismicity sources that affect the two sites of interest (point 1 and point 2 of Figure 1). In both cases, there are a large number of faults and background sources with negligible contributions to the seismic hazard. In fact the number of faults with significant contributions to the hazard at each point is rather small.

Seismic hazard in the case of site 1 is dominated by the Anthemountas fault at medium to large values of PGA, as should have been expected, due to the proximity of this point to the aforementioned fault. This fault is the only contributor to seismic hazard for values of PGA around 100 cm/sec^2. Background source XI, that represents the small earthquakes of the area which are not connected with the seismicity of any of the well defined faults, appears the largest contributor for small values of PGA. Finally, the Volvi, Stivos and Sohos faults mainly and Ierissos fault in a lesser extent, show around equal contributions to hazard for small to medium values of PGA.

The case of site 2 is different. Instead of lying in the proximity of a single fault, as is the case for point 1, this particular point lies at around equal distances from 3 different faults (Stivos, Anthemountas and Sohos). This fact is depicted in Figure 3 where it can be seen that the three aforementioned faults show around the same contribution to the hazard for this point. Again, background area source XI dominates the hazard for low values of PGA. At the same low range of PGA values, the contribution of the Volvi fault is also significant.

The next step of this analysis was the deaggregation of seismic hazard. During this procedure, the pair of magnitude and distance values that show the largest contribution to the hazard at the particular site can be determined. This pair (or pairs in case there exist more than one maxima) of M-R values may be assumed that comprise the most probable earthquake scenario for the specific site. The deaggregation was carried out for two values of return periods, 50 and 475 years. The results are shown in Figure 4.
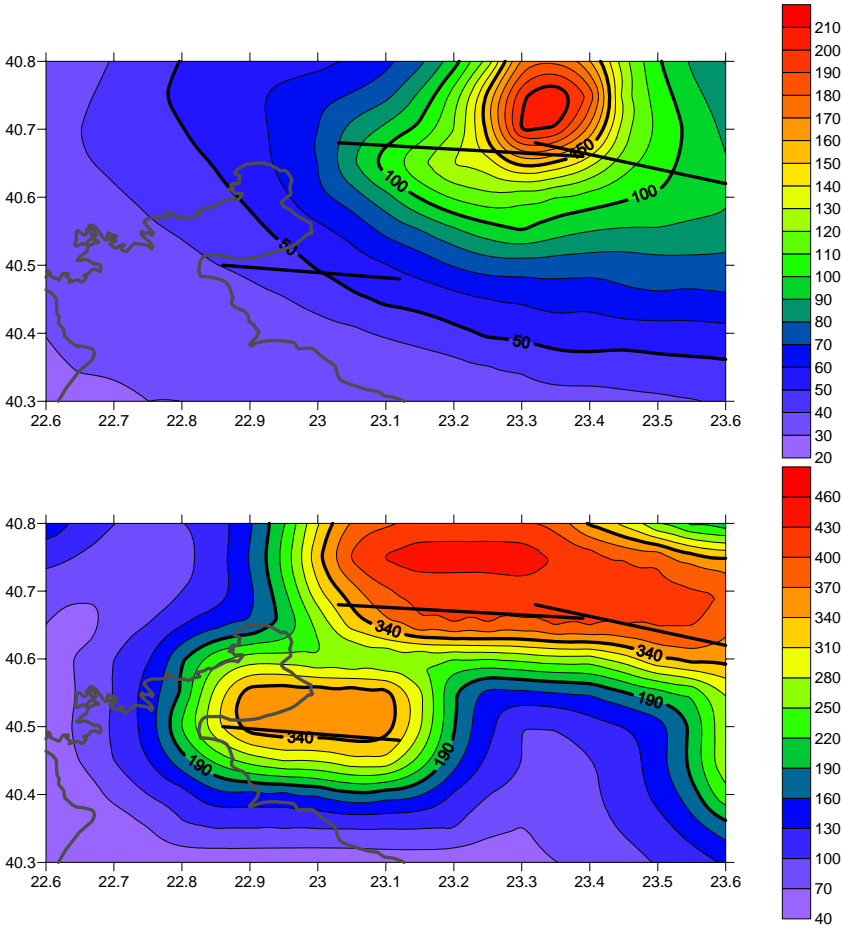
Figure 2. Distribution of expected PGA values at the study area, for two different values of return period, 50 years (top) and 475 years (bottom).

In the case of site 1, the return period of 50 years represents an expected PGA value of 51 cm/sec^2. From Figure 4 can be observed that for this value of PGA the largest contribution to the hazard is derived from the fault of Anthemountas, but almost equally significant is the contributions from the faults of Sohos and Stivos and to a lesser extent the one from Volvi. The results of the deaggregation confirm these conclusions. The maximum contribution appears at M=6.05 and R=32.5 km. Both faults of Sohos and Stivos lie at around this distance from point 1 and so this maximum represents their combined contribution. Another significant contribution at M=6.05 and R=2.5 represents the contribution of the Anthemountas fault. Some small contributions to the hazard exist for magnitudes of less than 6 and very small distances, which represent background area source IX.

The return period of 475 years represents an expected PGA value of 358 cm/sec^2 and from Figure 3 can be seen that at this value the total hazard is contributed by the Anthemountas fault. The same conclusion can be drawn from Figure 4 where only a single maximum can be observed at distances
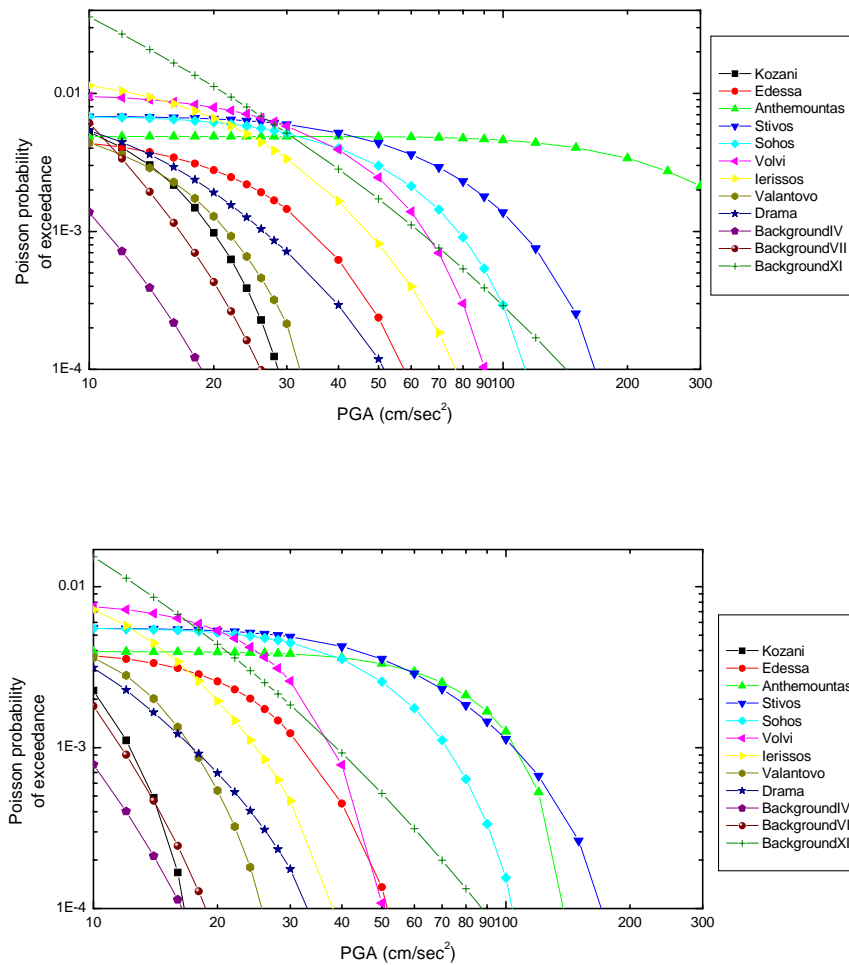
Figure 3. Contribution to the PGA hazard of point 1 (top) and point 2 (bottom) of the various faults and area sources of the area.

that are approximately equal to the distance between site 1 and Anthemountas fault (M=6.05 and R=2.5 km).

In the case of site 2, the return period of 50 years represents an expected PGA value of 55 cm/sec^2. For this value of PGA, the major contribution to the seismic hazard results from the combined contribution of the Anthemountas and Stivos faults with a smaller contribution from the Sohos fault (Figure 3). Indeed, the same conclusion can be drawn from Figure 4. The maximum contribution appears at M=6.15 and R=12.5 km which is approximately the minimum distance between site 2 and both Anthemountas and Stivos faults. There is also a smaller contribution at a distance of around 20 km, which represents the Sohos fault. The return period of 475 years represents an expected PGA value of 167 cm/sec^2 and in Figure 3 can be observed that the total amount of hazard is derived from the combined contribution of Anthemountas and Stivos faults. Again, the same conclusion can be drawn from Figure 4, where the unique and maximum contribution is located at M=6.25 and R=12.5. This distance represents approximately the minimum distance between site 2 and the two aforementioned faults.
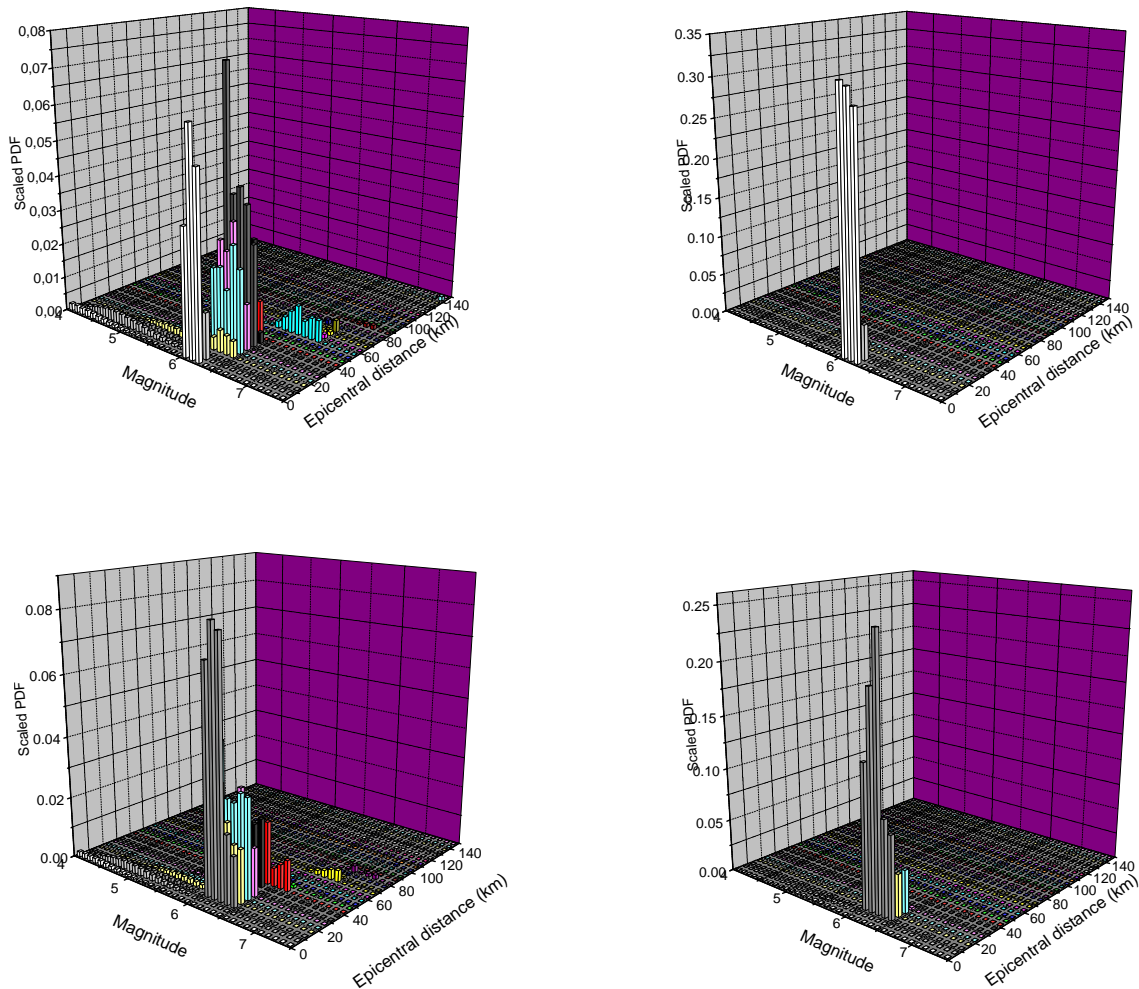
Figure 4. Deaggregation results for points 1 (top row) and 2(bottom row) and for two values of return period, 50 years (left column) and 475 years (right column).

Time histories are then estimated through the SmSim (Boore, 1996) code, based on point source ground motion model (PSM). The stochastic ground motion model (PSM), in which the energy is distributed randomly over the duration of source and path, has proven remarkably effective in correlating with a wide range of ground motion observations. Time-domain measures such as peak acceleration, velocity, Wood-Anderson magnitudes as well as frequency domain measures such as relative velocity response and Fourier amplitude spectra have been predicted with reasonable accuracy (Boore and Joyner; 1991; 1997). The ground motion model employed here uses a ω-square Brune source model (Brune, 1970; 1971) with a single corner frequency and a constant stress parameter (Boore, 1983). This methodology has been used in various applications in Greece (Margaris and Boore, 1998; Margaris and Hatzidimitriou, 2004).

This model estimates the times series and spectral values for each examined site utilizing the parameters of the faults and background area sources (Figure 1), which are given in the EUROSEISRISK report (Margaris and Koutrakis, 2004). Considering the deaggregation results (Figure 4) and the estimated M-R pairs time histories and 5% pseudoacceleration spectral values are computed. The appropriate input parameters of PSM model have been presented in the same aforementioned report proposed by Margaris and Koutrakis (2004). Figure 5 depicts the PGA and 5% PSA spectral values based on the deaggregation pairs of magnitude and distance, M-R, for each examined site of the probabilistic seismic hazard assessment.
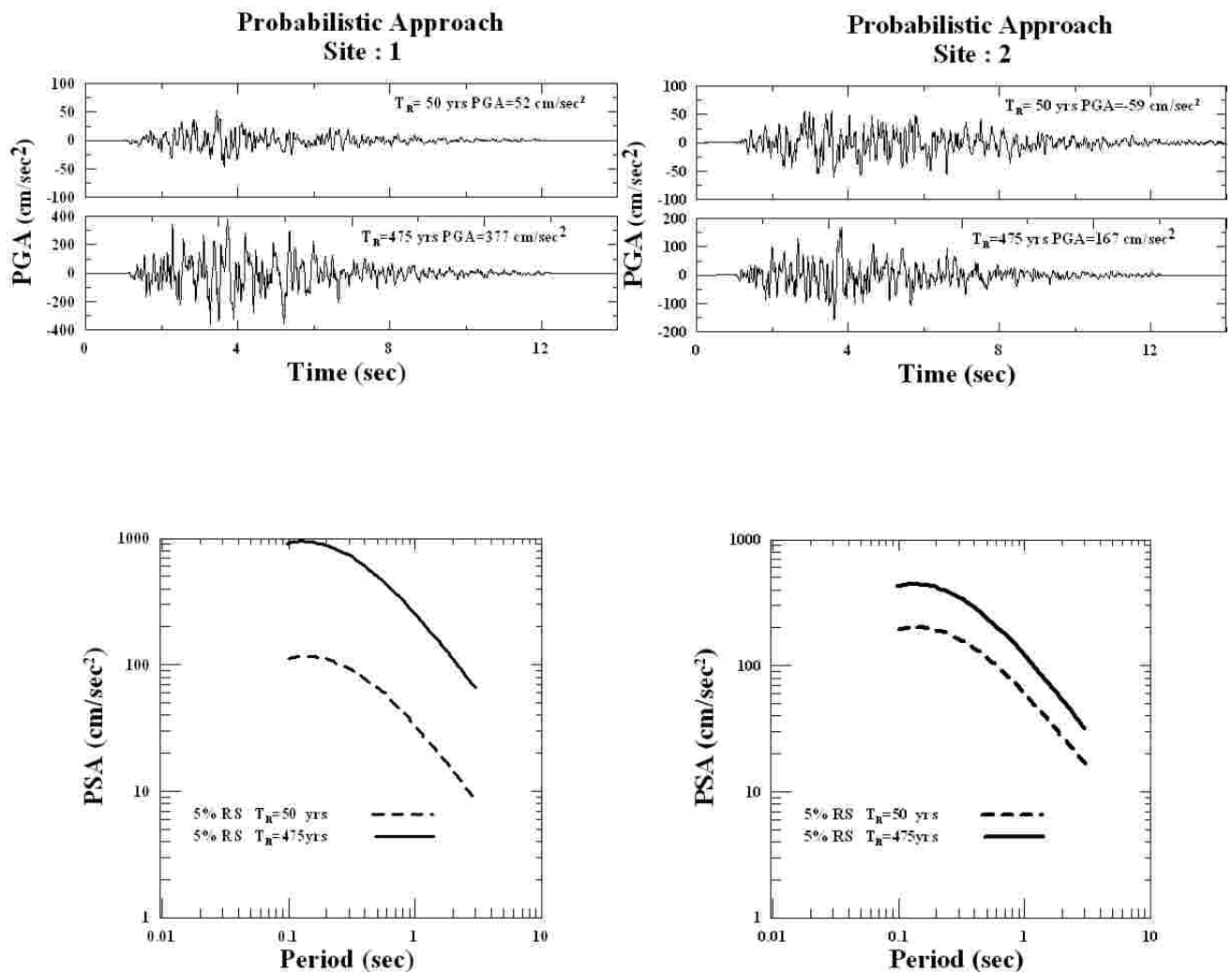
Figure 5. Simulated time histories and spectral values for the two examined sites, based on de-aggregation results.

Deterministic approach

The deaggregation performed at sites 1 and 2 showed that Stivos fault largely contributes to the hazard for expected PGA values at 50 and 475 years return periods. These sites have a fault distance within 2 times the fault length, and they can experience ground shaking affected by the details of the rupture propagation on the fault, such as directivity effects. A hybrid stochastic-deterministic technique (DSM-Deterministic-Stochastic Method; Pacor et al., 2005) was then used to compute the high-frequencies (f>0.5-1 Hz) ground motions due to extended fault. DSM allows computing synthetic time series for direct S-wave field at bedrock sites, and is suitable to generate shaking scenarios near an extended fault whereby the direct S wave-field is generally dominant in amplitude with respect to the reflected and superficial phases. Different rupture propagation models on the selected faults can be hypothesized and, even when input data regarding earthquake source, propagation medium, and site characteristics are of a very schematic nature, the complexity of near-source ground motion can be adequately reproduced. Extended fault simulations performed with different, but equally probable, rupture models generally produce a high variability in the ground motion, mainly dependent on the assumed position of the hypocenter on the fault plane, which controls the rupture directivity.

Several ground motion scenarios have been performed in the Thessaloniki area within the LessLoss EU project (Deliverable 80, 2005). The 1D crustal model for S-waves velocity was inferred from the

3D tomographic image of the crust-uppermost mantle in the Aegean area using the group velocities of Rayleigh wave fundamental mode (Karagianni et al., 2005); P-velocities and density results from Papazachos and Nolet (1997), with the exception of the first layer of the model which was taken from project RISK-UE (Table 1) (Karagianni, personal communication; Pitilakis et al., 2004). The spectral attenuation was defined in terms of quality factor Q and diminution parameter ko, which controls the high-frequency decay of the spectrum. We used Q(f) = 88 f 0.9, in good agreement with Q values obtained with data from local earthquakes that occurred in the Thessaloniki area (Hatzidimitriou, 1995), and the diminution parameter ko=0.035s as suggested by Margaris and Boore (1998). This value ko was considered as representative of class A sites and it was employed to perform bedrock simulations.

Table 1. 1D crustal model for the studied area

Depth (km)	Vp (km/s)	Vs (km/s)	Rho (g/cm^3)
0	4.5	2	2.4
1	6.06	3.44	2.7
5	6.07	3.46	2.8
11	6.37	3.64	2.9
21	6.96	3.98	3
31	7.64	4.36	3.2

The fault geometry was taken from the geodetic study of Stiros and Drakos (2000), as in Table 2 and Figure 6. Deterministic shaking scenarios for Stivos fault have been computed for a uniform slip distribution on a normal fault with bilateral rupture starting from the hypocenter location. The simulations were done considering the variability of the kinematic source parameters (e.g. rupture velocity and nucleation point). Three different rupture velocities were assumed on the fault, corresponding to 75%, 80% and 90% of shear-weave velocity (VR =2.625, 2.8 and 3.15 km/s).
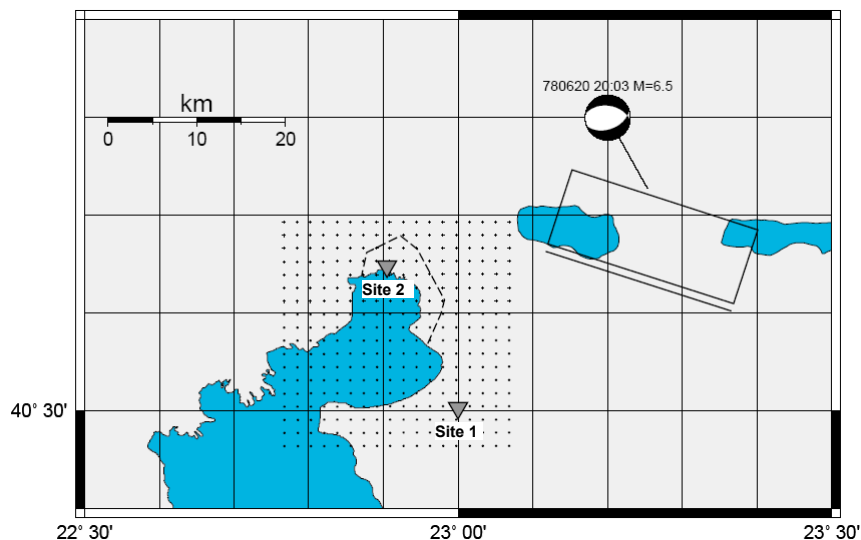

Figure 6 - Position and dimension of the1978 source fault. The focal mechanisms of 1978 earthquake and of the two main aftershocks are also reported. Site 2 is close to THE accelerometric station. Triangles indicate the grid points where the synthetic time series were simulated.

Table 2. Fault parameters

Fault	M	Mo (dyne.cm)	LxW (km^2)	<Δu> (cm)	Strike (deg)	Dip (deg)	Ztop (km)
Stivos, 1978 Thessaloniki eq	6.5	6.3 x 10^{25}	22 x 14	59	288°	51°	1.1

Figure 7 shows the PGA maps obtained by considering the minimum and the maximum values of the hypothesized VR. Both scenarios represented in Figure 7 are influenced by the source location respect to the Thessaloniki area and by directivity effects. In fact, increasing values of PGA can be observed as source-to-site distance decreases from West to East. Peak accelerations ranging from 30 to 60 gals or from 50 to 100 gals are obtained in Thessaloniki area depending on the assumed rupture velocity.
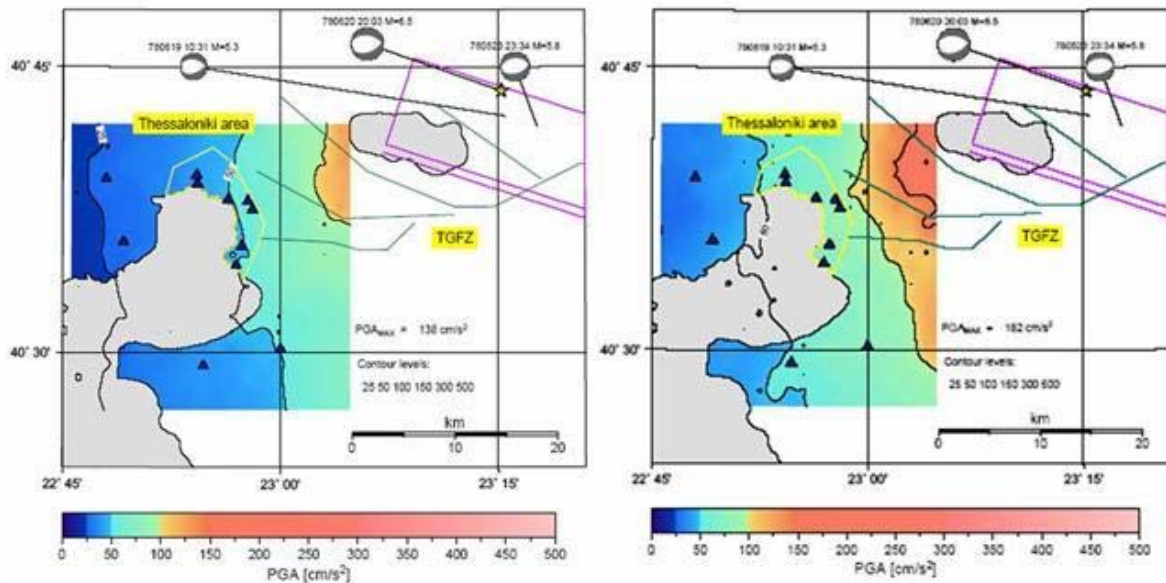

Figure 7. PGA values on the Thessaloniki metropolitan and surrounding area (bedrock scenarios) for the 1978 Thessaloniki earthquake with VR = 2.625 km/s (left panel) and VR = 3.150 km/s (right panel).

In order to verify the input parameters for modeling, such as crustal model and rupture velocity on the fault, we tried to reproduce the wave field of the 1978 Thessaloniki earthquake (M=6.5). The Gerakarou-Stivos fault is associated to the June 20, 1978 Thessaloniki earthquake with the epicentre located at a distance of about 25 km NE from the city (Stiros and Drakos, 2000 and references therein). Moreover, the earthquake was recorded by one accelerometric station (THE-City Hotel, Figure 6) located in the basement of an eight-story building at the shoreline of the city (PGA ~0.15g; Pitilakis et al., 2004).

The accelerogram recorded at the THE-City Hotel station was compared with synthetic time series, considering an average value of rupture velocity (VR =2.8 km/s) and introducing the combined effects of site amplification and attenuation. We considered the representative transfer function of class C sites and assumed ko=0.056 s (Margaris and Boore, 1998). Figure 8 shows the horizontal components of recorded and simulated accelerations at station THE-City Hotel. Synthetics are performed to reproduce only the stronger of the two sub-events as they are separated in Margaris and Boore (1998). The waveform comparison shows that the strong motion phase is rather well reproduced both in amplitude and shape, although synthetic accelerations appear to be more reach than recorded in the high frequency content.
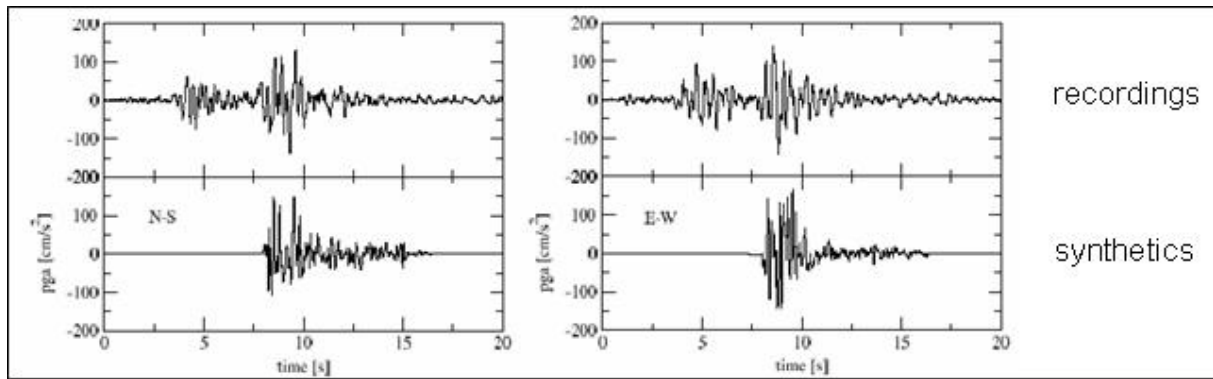
Figure 8. Waveforms comparison at station THE: left panel, North-South component; right panel, East-West component. The accelerogram recorded at the THE-City Hotel station in downtown Thessaloniki shows the double event of June 20, 1978, earthquake (M=6.5).

DISCUSSIONS AND CONCLUSIONS

The probabilistic approach accounts for the likelihood that a range of small and large earthquakes may occur along the seismic faults and seismic sources in the broader area of the two examined sites. It combines information on earthquake size, location and probability of occurrence with the resulting ground motion to give results in terms of PGA and the associated annual probability of exceedance. In addition to this, deaggreagation analysis is attempted and the most probable M-R pair from seismic sources and faults affecting the two examined sites is defined.

The deterministic approach is justified for specific and major seismic faults generating characteristic earthquakes of similar size. In the hybrid stochastic-deterministic technique (DSM: Deterministic-Stochastic Method) the target earthquakes are usually selected through considerations on historical seismicity and geological and physical characteristics of the seismic sources. This methodology more realistically approaches characteristics of the extended faults and describes the near-field effects on ground motion.

Figures 9 and 10 show the comparison of time series and spectral acceleration obtained from the two different approaches applied to sites 1 and 2: the DSM simulations for the 1978 Thessaloniki earthquake (two horizontal components, NS and EW) and the SmSim synthetics associated to the magnitude-distance bins of the deaggregation results (two return periods, TR=475 and 50 years).

The deaggregation defined the most probable design magnitude and distance (M-R bin) for the two return periods, taking into account all the seismic sources in the broader area which actively affect the examined sites. The resulting distance allowed then the identification of the closest probable seismic sources (fault or area), which mainly contribute to seismic hazard of each site. However, the SmSim ground motions refer to a point source located at the defined distance from the site. For site 1 the maximum contribution to PGA with Tr=50 years return period (Figure 9, bottom time series to the right) is due to M=6.05 and R=32.5 km, which can be related to Sohos and Stivos faults. Moreover, for site 2 (Figure 10) both return periods individuate sources at distance R=12.5km (combined contribution of Anthemountas and Stivos faults) but with M=6.25 (Tr=475y) and M=6.15 (Tr=50y).

The DSM model estimated synthetic ground motions for the M=6.5, 1978 Thessaloniki earthquake, which ruptured the Stivos fault. The DSM synthetics are more realistic in time and frequency domain taking into account the kinematic behavior of the rupture on extended fault and 1-D propagation effects (Figure 9 and 10). However, the deterministic approach do not account for the seismic activity of the broader examined area and its likelihood occurrence, while the probabilistic approach estimates only mean reliable ground motion values without using refined source, path and site parameters.

The discrepancies of the two approaches are depicted by the spectral value comparisons in the bottom plot of Figures 9 and 10. These discrepancies are due to different approaches of the estimate of ground motion which produces different seismic scenarios for the two points (1&2) and in some minor differences in the seismotectonic settings adopted in two approaches. For example, in the DSM simulation the hypocenter of the extended source earthquake refers to the one of 1978 earthquake, i.e. about 30 km far from the 2 sites, whereas in the SmSim simulations the point source is about 13 km from site 2 and it can be approximated as a nucleation point located a left edge of the fault (closest distance from site to fault).

Both methodologies can be reliably used to estimate potential earthquakes for which no strong-motion records from similar historical seismic events exist. Moreover, synthetics may be prove useful for filling gaps in empirical data.
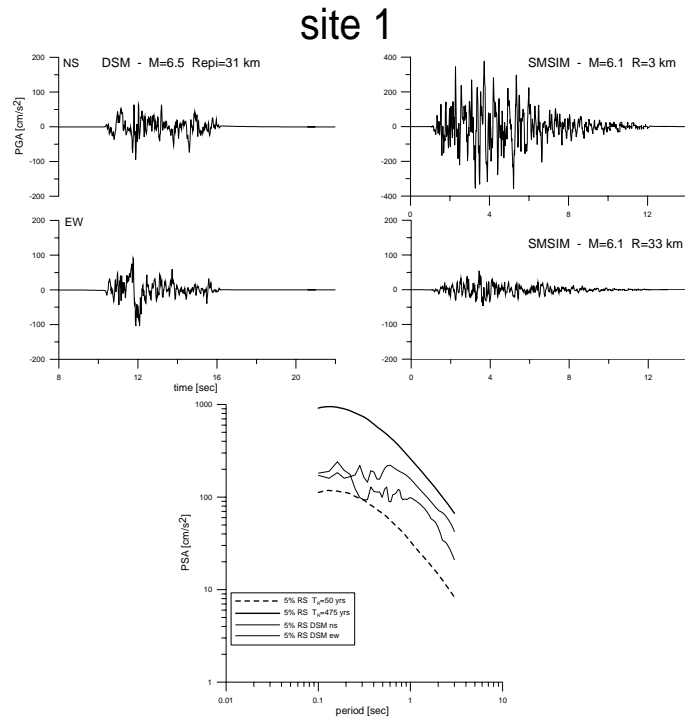
site 1

Figure 9. Comparison of the simulations based on two approaches for the examined site 1: Left column (up) -DSM simulation of Thessaloniki 1978 seismic event, M 6.5 (NS and EW components) and right column (up) -SmSim simulation for M-R referred to two return periods, TR=475 (top) and 50 years (bottom); spectral values from the simulated time series (bottom).
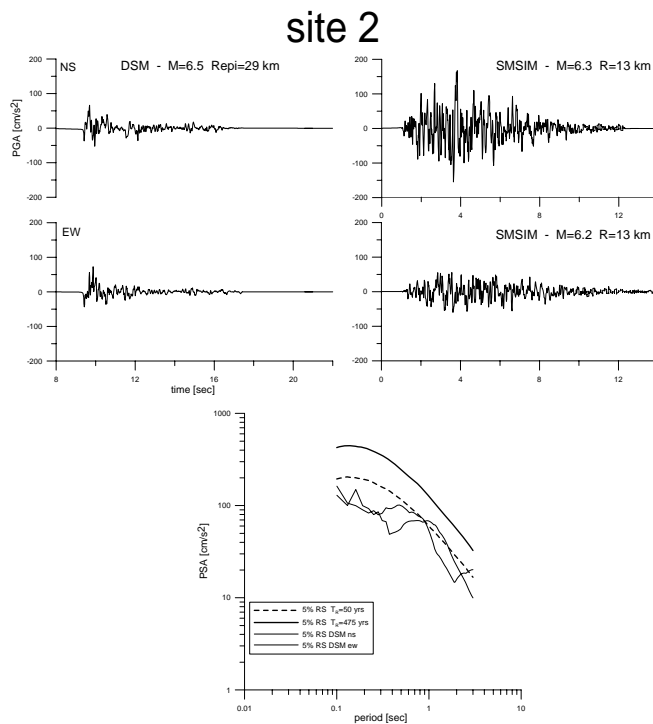
site 2

Figure 10. Comparison of the simulated time histories and spectral values for the examined site 2 based on two approaches (see Figure 9)

REFERENCES

Ambraseys, N.N., Douglas, J., Sarma, S.K., Smit, P.M. "Equations for the estimation of strong ground motions from shallow crustal earthquakes using data from Europe and Middle East: Horizontal peak ground acceleration and spectral acceleration", Bull. of Earthquake Engineering, 3, 1-53, 2005.

Boore, D.M. "Stochastic simulation of high-frequency ground motions based on seismological models of the radiated spectra", Bull. Seism.. Soc. Am.,73, 1865-1894, 1983.

Boore, D.M. and W.B. Joyner. "Estimation of ground motion at deep-soil sites in Eastern North" America, Bull. Seism.. Soc. Am., 81, 2167-2185, 1991.

Boore, D.M. and W.B. Joyner. "Site amplifications for Generic rock sites", Bull. Seism.. Soc. Am., 87, 327-341, 1997.

Boore, D.M., Joyner, W.B., Fumal, T.E. (1997). "Equations for estimating horizontal response spectra and peak acceleration from Western North American earthquakes: a summary of recent work", Seismological Research Letters, 68(1), 128-153.

Brune, J.N. "Tectonic stress and the spectra of seismic shear waves from earthquakes", J. Geoph. Res., 75, 4997-5009, 1970.

Brune, J.N. " Correction", J. Geoph. Res., 76, 5002, 1971.

Deliverable 80 – Technical report on the scenario earthquake definition for three cities. LessLoss Project: Risk Mitigation for Earthquakes and Landslides Integrated Project, Sixth Framework Programme Project No.: GOCE-CT-2003-505488, Sub-Project 10: Disaster scenarios prediction and loss modelling for urban areas. September, 2005.

Karagianni, E.E., Papazachos, C.B., Panagiotopoulos, D.G., Suhadolc, P., Vuan, A., Panza, G. F. (2005) "Shear velocity structure in the Aegean area obtained by inversion of Rayleigh waves", Geophysical Journal International, 160(1), pp. 127-143.

Margaris B.N. and Boore D.M. "Determination of $\Delta\sigma$ and $\kappa 0$ from response spectra of large earthquakes in Greece, Bull. Seism. Soc. Am. 88, 170–182, 1998.

Margaris, B.N. and Hatzidimitriou, P.M. "Source spectral scaling and stress release estimates using strong motion records in Greece", Bull. Seism. Soc. Am. 92, 1040–1059, 2002.

Margaris, B. N. and Koutrakis, S. I. "Probabilistic and Deterministic Seismic Hazard Studies in the Area using Different Methodologies (D20) and Evaluation of Seismic Hazard of the Area. Earthquake Scenarios of Ground Motion Studies (D21)", EUROSEISRISK Final Report, 2004.

Pacor, F., Cultrera, G., Mendez, A. , Cocco, M. (2005). "Finite Fault Modeling of Strong Ground Motion Using a Hybrid Deterministic - Stochastic Method", Bull. Seism. Soc. Am., 95, 225-240.

Papazachos, B.C., Papazachou, C. (1997) "The Earthquakes of Greece," Ziti Publications, Thessaloniki.

Papazachos, B.C., Mountrakis D. M., Papazachos C. B., Tranos M. D., Karakaisis G. F. and Savvaidis A. S. "The faults which have caused the known major earthquakes in Greece and surrounding region between the 5th century BC and today," Proc. 2nd Hell. Congress on Earthquake Eng. and Eng. Seism., Thessaloniki, 28-30 Nov. 2001, A, 17-26, 2001

Papazachos, C., Nolet, G., (1997) "P and S deep velocity structure of the Hellenic area obtained by robust nonlinear inversion of travel times", J. Geophys. Res., 102, pp. 8349– 8367.

Pitilakis, K., (2004) "Chapter 5: Site effects", Recent Advances in Earthquake Geotechnical Engineering & Microzonation, A. Ansal ed., Kluwer Publ.

Skarlatoudis, A. A., Papazachos C. B., Margaris B. N., Theodulidis N., Papaioannou Ch., Kalogeras I., Scordilis E. M., and Karakostas V. "Empirical Peak Ground-Motion Predictive Relations for Shallow Earthquakes in Greece," Bull. Seism. Soc. Am., 93, 2591-2603, 2003.

Stiros, S.C., Drakos, A. (2000) "Geodetic constrain on the fault pattern of the 1978 Thessaloniki (Northern Greece) earthquake (MS=6.4) " , Geophys. J. Int. (2000), 143, 679-688.

Tranos, M.D., Papadimitriou, E.E., Kilias, A.A. (2003). "Thessaloniki–Gerakarou Fault Zone (TGFZ): the western extension of the 1978 Thessaloniki earthquake fault (Northern Greece) and seismic hazard assessment", Journal of Structural Geology 25, 2109–2123.

Tromans I.J., Bommer J.J. (2002). "The attenuation of strong-motion peaks in Europe", Proceedings of the Twelfth European Conference on Earthquake Engineering, London, Paper No. 394

Wells, D.L., Coppersmith, K.J. (1994). "New empirical relationships among magnitude, rupture length, rupture width, rupture area, and surface displacement", Bull. Seism. Soc. Am., 84, 974-1002.